

## Excited-State Double Proton Transfer in 7-Azaindole Analogues: Observation of Molecular-Based Tuning Proton-Transfer Tautomerism

Pi-Tai Chou,\* Ching-Yen Wei, Go-Ray Wu, and Wen-Sin Chen

Department of Chemistry  
The National Chung-Cheng University  
Chia-Yi, Taiwan, R.O.C.

Received May 27, 1999

Revised Manuscript Received August 21, 1999

Self-dimerization of 7AI has long been recognized for undergoing the excited-state double proton transfer (ESDPT) resulting in a large Stokes shifted emission.<sup>1a–m</sup> Such a simple ESDPT process provides one possible mechanism for the mutation due to a “misprint” of a specific DNA base pair.<sup>1b,h</sup> Further focus on the ESDPT reaction relevant to the molecular nature of mutation requires the study of the proton-transfer reaction in 7AI analogues of biological importance, among which, purines possessing a similar structural moiety are particularly crucial.

Purine has been found to exist predominantly as an N(9)H tautomeric form in the gas phase as well as isolated inert matrices,<sup>2</sup> while there exists an equilibrium mixture of N(7)H and N(9)H tautomers in protic solvents<sup>3</sup> (see Figure 1). However, the tautomeric reaction regarding the proton migration to the N(3) position has not yet been reported. Our approach is to systematically investigate the ESDPT reaction on a molecular basis in which a nitrogen atom is first added to the five-membered ring of 7AI, forming 4-azabenzimidazole (4ABI). Subsequently, 6-isobutylpurine (6IBP,<sup>4</sup> Figure 1) was synthesized to study the comparative proton-transfer tautomerism.<sup>6</sup>

Significant concentration-dependent absorption spectra<sup>6</sup> were observed for both 4ABI and 6IBP (see Figure 2). For the case of 4ABI, the 287 nm peak characterized for the monomer<sup>7</sup> gradually disappears upon increasing the concentration, accompanied by a

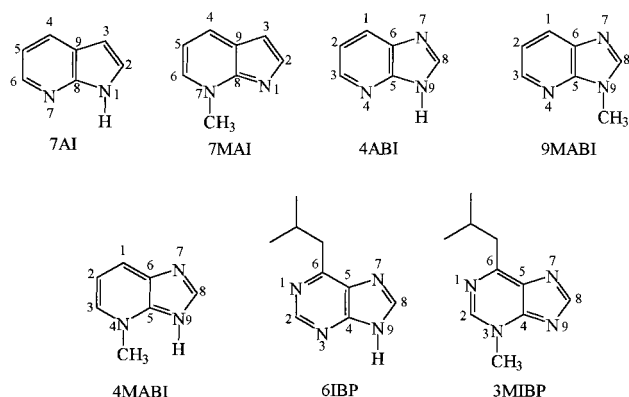
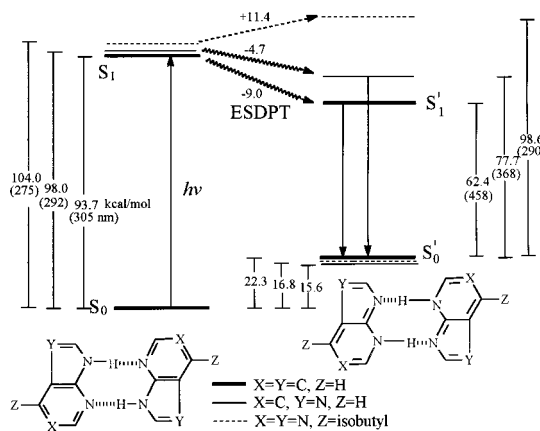


**Figure 1.** Structures of 7AI, 4ABI, 6IBP, and their methylated derivatives.

### Scheme 1



red shift of the overall spectrum and an appearance of a shoulder at 292 nm. In comparison, N(9)-methyl-4-azabenzimidazole (9MABI),<sup>8</sup> which is treated as a non-proton transfer model, shows concentration-independent absorption profiles (see Table 1). The results unambiguously conclude the occurrence of self-aggregation for 4ABI. A straight-line plot for  $C/A_{300}$  vs  $(1/A)^{1/2}$  (see insert of Figure 2A) supports a dominant dimeric formation. Similar behavior was also observed for 6IBP (see insert of Figure 2B). Accordingly, the association constant,  $K_a$ , was calculated to be  $\sim 3.0 \times 10^3$  and  $4.2 \times 10^3 \text{ M}^{-1}$  for 4ABI and 6IBP, respectively, in  $\text{CCl}_4$  (305 K).

At sufficiently low concentrations so that only 4ABI monomer exists, a normal Stokes-shifted emission was observed with a peak maximized at 308 nm. Dual fluorescence was observed upon increasing the concentration, consisting of a 308 nm emission (the  $F_1$  band,  $\tau_f \approx 0.32$  ns) followed by a large Stokes-shifted emission maximum at 380 nm (the  $F_2$  band,  $\tau_f = 2.04$  ns). The excitation maximum ( $\sim 292$  nm) monitored at the  $F_2$  band was red-shifted by  $\sim 5$  nm with respect to that monitored at the  $F_1$  band. The results in combination with the system-response rise time ( $< 3 \times 10^{-10}$  s) for both components lead us to conclude the two emitting bands originate from two distinct ground-state

(8) 9MABI was synthesized by treating 4ABI with NaH and  $\text{CH}_3\text{I}$  in a ratio of 1:2:2 in dry THF at  $0^\circ\text{C}$ .  $^1\text{H NMR}$  ( $\text{D}_2\text{O}$ , 400 MHz)  $\delta$  3.87(s, 3H); 7.31(m, 1H); 8.03(d,  $J = 8.0$  Hz, 1H); 8.23(s, 1H); 8.29(d,  $J = 4.0$  Hz, 1H).

(9) Equation 1

$$\frac{C}{A} = \frac{1}{\epsilon} + \left( \frac{1}{2\epsilon K_a} \right)^{1/2} \left( \frac{1}{A} \right)^{1/2} \quad (1)$$

has been derived for the monomer–dimer association<sup>1b,g,l</sup> where  $C$  denotes the prepared concentration,  $A$  is the absorbance of the dimer at a selective wavelength,  $\epsilon$  is the molar extinction coefficient of the dimer, and  $K_a$  is the association constant.

\* To whom correspondence should be addressed.

(1) (a) Taylor, C. A.; El-Bayoumi, A. M.; Kasha, M. *Proc. Natl. Acad. Sci. U.S.A.* **1969**, *65*, 253. (b) Ingham, K. C.; El-Bayoumi, M. A. *J. Am. Chem. Soc.* **1974**, *96*, 1674. (c) Fuke, K.; Yoshiuchi, H.; Kaya, K. *J. Phys. Chem.* **1984**, *88*, 58402. (d) Tokumura, K.; Watanabe, Y.; Udagawa, M.; Itoh, M. *J. Am. Chem. Soc.* **1987**, *109*, 1346. (e) Chapman, C. F.; Maroncelli, M. *J. Phys. Chem.* **1992**, *96*, 8430. (f) Chen, Y.; Gai, F.; Petrich, J. W. *J. Am. Chem. Soc.* **1993**, *115*, 10158. (g) Chou, P. T.; Wei, C. Y.; Chang, C. P.; Kuo, M. S. *J. Phys. Chem.* **1995**, *99*, 11994. (h) Douhal, A.; Kim, S. K.; Zewail, A. H. *Nature (London)* **1995**, *378*, 260. (i) Smirnov, A. V.; English, D. S.; Rich, R. L.; Lane, J.; Teyton, L.; Schwabacher, A. W.; Luo, S.; Thornburg, R. W.; Petrich, J. W. *J. Phys. Chem. B* **1997**, *101*, 2758. (j) Chachisvillias, M.; Fiebig, T.; Douhal, A.; Zewail, A. H. *J. Phys. Chem. A* **1998**, *102*, 669. (k) Chou, P. T.; Yu, W. S.; Chen, Y. C.; Wei, C. Y.; Martinez, S. S. *J. Am. Chem. Soc.* **1998**, *120*, 12927. (l) Takeuchi, S.; Tahara, T. *J. Phys. Chem. A* **1998**, *102*, 7740. (m) Catalan, J.; Del Valle, J. C.; Kasha, M. *Proc. Natl. Acad. Sci. U.S.A.* **1999**, *96*, 8338.

(2) (a) Lin, J.; Yu, S.; Peng, S.; Akiyama, I.; Li, K.; Lee, L. K.; LeBreton, P. R. *J. Am. Chem. Soc.* **1980**, *102*, 4627. (b) Wiorcikiewicz-Kuczera, J.; Karplus, M. *J. Am. Chem. Soc.* **1990**, *112*, 5324. (c) Nowak, M. J.; Rostkowska, H.; Lapinski, L.; Kwiatkowski, J. S.; Leszczynski, J. *J. Phys. Chem.* **1994**, *98*, 281326.

(3) (a) Pugmire, R. J.; Grant, D. M. *J. Am. Chem. Soc.* **1971**, *93*, 1880. (b) Dryefus, M.; Dodin, G.; Bensaude, O.; Dubois, J. E. *J. Am. Chem. Soc.* **1975**, *97*, 2369. (c) Chenon, M. T.; Pugmire, R. J.; Grant, D. M.; Panzica, R. P.; Townsend, L. B. *J. Am. Chem. Soc.* **1975**, *97*, 4636. (d) Gonnella, N. C.; Roberts, J. D. *J. Am. Chem. Soc.* **1982**, *104*, 3162. (e) Holmen, A.; Broo, A.; Albinsson, B.; Norden, B. *J. Am. Chem. Soc.* **1997**, *119*, 12240.

(4) 6IBP was used due to its high solubility in nonpolar solvents and the feasibility of synthesizing the N(3) tautomer. 6IBP was synthesized according to ref 5.  $^1\text{H NMR}$  ( $\text{CDCl}_3$ , 200 MHz)  $\delta$  1.01 (d, 6H,  $J = 6.6$  Hz); 2.27–2.54 (m, 1H); 3.13 (d, 2H,  $J = 7.2$  Hz); 8.25 (s, 1H); 8.96 (s, 1H).

(5) Dvorakova, H.; Dvorak, D.; Holy, A. *Tetrahedron Lett.* **1996**, *37*, 1285.

(6) Steady-state absorption and emission spectra were recorded by a Cary 3E (Varian) spectrophotometer and a Hitachi (SF4500) fluorimeter, respectively.

(7) Similar to the predominant N(9) form of various purines in inert matrices<sup>2</sup> both 4ABI and 6IBP exist predominantly in their N(9)H forms in nonpolar solvents.

**Table 1.** Thermodynamic and Photophysical Properties of 7AI, 4ABI, 6IBP, and Their Methylated Derivatives in Cyclohexane and CCl<sub>4</sub><sup>a</sup>

	absorption (nm)	emission (nm)	$\Phi_f$	$\tau_f$ (ns)	$K_a$ (M <sup>-1</sup> )
7AI	(287, 293 <sup>sh</sup> )	320	0.22 <sup>c</sup>	1.68 <sup>b</sup> , 1.72 <sup>c</sup>	
7AI dimer	(292, 305 <sup>sh</sup> ) <sup>e</sup>	480	0.016	2.82 <sup>b</sup> , 3.0 <sup>d</sup>	2.2 × 10 <sup>3</sup> <sup>f</sup> 5.2 × 10 <sup>2</sup> <sup>b,g</sup>
7MAI	(390, 458 <sup>sh</sup> )	(463 <sup>sh</sup> , 495, 510)	0.0066 <sup>b</sup> 0.0073 <sup>c</sup>	1.54, 1.67 <sup>c</sup>	
4ABI	(281, 287)	306	0.038	0.44	
4ABI dimer	(282, 287) <sup>b</sup> (285, 292) <sup>e</sup> (285, 292) <sup>b,e</sup>	308 <sup>b</sup> 380 380 <sup>b</sup>	0.012 <sup>b</sup> 0.05 0.06 <sup>b</sup>	0.32 <sup>b</sup> 1.19 2.04 <sup>b</sup>	3.0 × 10 <sup>3</sup> <sup>b</sup>
4MABI	(292, 329, 368 <sup>sh</sup> ) (292, 330, 368 <sup>sh</sup> ) <sup>b</sup>	(372 <sup>sh</sup> , 400) (372 <sup>sh</sup> , 400) <sup>b</sup>	0.031 0.053 <sup>b</sup>	1.80 2.60 <sup>b</sup>	
9MABI	(284, 290) (284, 292) <sup>b</sup>	305 308 <sup>b</sup>	0.014 0.020 <sup>b</sup>	0.48 0.50 <sup>b</sup>	
6IBP	263, 263 <sup>b</sup>	—	—	—	
6IBP dimer	(267, 275 <sup>sh</sup> ) <sup>b</sup>	—	—	—	4.2 × 10 <sup>3</sup> <sup>b</sup>
3MIBP	(266, 275, 287 <sup>sh</sup> ) (268, 312, 290 <sup>sh</sup> ) <sup>b</sup>	(290 <sup>sh</sup> , 310) (290 <sup>sh</sup> , 315)*	0.018 0.025	0.63 0.70	

<sup>a</sup> sh: shoulder. <sup>b</sup>In CCl<sub>4</sub>. <sup>c</sup>Reference 1e. <sup>d</sup>Reference 1d. <sup>e</sup>Obtained from the fluorescence excitation spectrum. <sup>f</sup>Reference 1g. <sup>g</sup>Reference 1b.

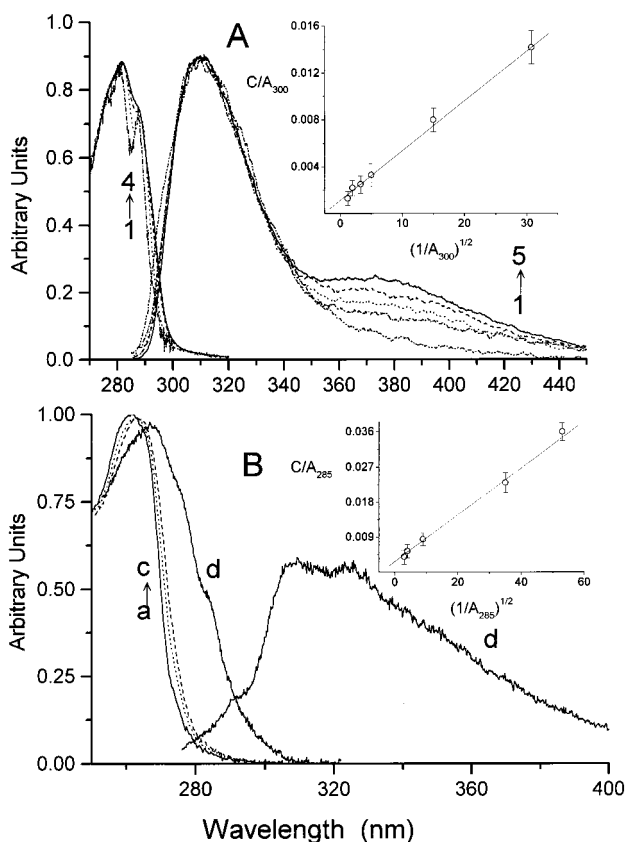


**Figure 2.** A. The absorption (normalized at 276 nm) and emission spectra of ( $\lambda_{\text{ex}} = 280$  nm) 4ABI at **1.**  $1.5 \times 10^{-5}$ , **2.**  $1.3 \times 10^{-4}$ , **3.**  $2.5 \times 10^{-4}$ , **4.**  $5.0 \times 10^{-4}$ , **5.**  $1.2 \times 10^{-3}$  M in CCl<sub>4</sub> (305 K). Insert: Plot of  $C/A_{300}$  values versus  $(1/A_{300})^{1/2}$  and a best least-squares fitting curve using eq 1.<sup>9</sup> To avoid spectral complexity only four curves were depicted in absorption spectra. B. The absorption spectra (normalized at 263 nm) of 6IBP at (a)  $1.2 \times 10^{-5}$ , (b)  $1.0 \times 10^{-4}$ , and (c)  $3.0 \times 10^{-4}$  M. Insert: Plot of  $C/A_{285}$  values versus  $(1/A_{285})^{1/2}$  and a best least-squares fitting curve. (d) The absorption and emission spectra ( $\lambda_{\text{ex}} = 270$  nm) of 3MIBP.

species in which the F<sub>1</sub> band originates from the non-hydrogen-bonded monomer. Consequently, the F<sub>2</sub> band can be ascribed to the N(4)H tautomer emission resulting from ESDPT. To further verify this viewpoint N(4)-methyl-4azabenzimidazole (4MABI) was synthesized,<sup>10</sup> which exhibits absorption onset and fluorescence maximum at 368 and 400 nm ( $\phi_f \approx 0.053$ ,  $\tau = 2.60$  ns in CCl<sub>4</sub>), respectively. The spectral resemblance (i.e., peak maxi-

(10) 4MABI was synthesized by forming the 4-methyl-4ABI salt with CH<sub>3</sub>I followed by deprotonation in strong basic conditions. <sup>1</sup>H NMR (D<sub>2</sub>O, 400 MHz)  $\delta$  4.23 (s, 3H); 7.28 (t,  $J = 7.1$  Hz, 1H); 8.07(d,  $J = 6.2$  Hz, 1H); 8.28(d,  $J = 5.2$  Hz, 1H); 8.29(s, 1H).

um, lifetime, etc.) between 4MABI and the F<sub>2</sub> band supports the occurrence of ESDPT in the 4ABI dimer. On the contrary, although  $K_a$  for the 6IBP dimer determined from the absorption spectroscopy is the greatest among the three 7AI analogues, no emission is detectable throughout 280–600 nm. For comparison, the N(3) methylated tautomeric form of 6IBP, N(3)-methyl-6-isobutylpurine (3MIBP)<sup>11</sup> exhibits an emission maximum at 325 nm with a spectral onset at  $\sim 290$  nm (see Figure 2B).

The photophysical properties shown in Table 1 reveal an interesting correlation between the energy gap and the corresponding number of nitrogen atoms in the methylated tautomers of 7AI, 4ABI, and 6IBP, in which a significant blue shift of the first peak on the order of N(7)-methyl-7azaindole (7MAI, 21 834 cm<sup>-1</sup>) < 4MABI (27 200 cm<sup>-1</sup>) < 3MIBP (30 770 cm<sup>-1</sup>) was observed. Thus, adding electron-rich nitrogen atoms in either a five- or six-membered ring of 7AI alters the tautomeric form toward an increase of the  $\pi \rightarrow \pi^*$  energy gap. Conversely, the differences in 0–0 onsets among normal dimers are relatively much smaller, being only 1460 and 3570 cm<sup>-1</sup> higher in energy than that of the 7AI dimer for 4ABI and 6IBP dimeric forms, respectively.<sup>13</sup> Using a 6-31G(d,p) basis set with the inclusion of solvation free energy (the PM3-SM4 method) for each species,<sup>14</sup> the formation free energy of 7AI, 4ABI, and 6IBP tautomer dimeric forms are calculated to be 22.3, 15.6, and 16.8 kcal/mol, respectively, relative to their corresponding normal dimers. It is rather difficult to assign the S<sub>0</sub>–S<sub>1</sub> (0–0) transition of the tautomer dimer due to either spectral overlap (in 4ABI) or the lack of the tautomer emission (in 6IBP). Simply, we took the absorption onset of their corresponding methylated tautomers shown in Table 1. Accordingly, ESDPT is calculated to be –9.0 and –4.7 kcal/mol exergonically for 7AI and 4ABI dimers, respectively. In contrast, a large endergonic value of 11.4 kcal/mol was obtained for the 6IBP dimer, indicating that the ESDPT reaction is thermally unfavorable.

In conclusion, the energy gap between S'<sub>0</sub> and S'<sub>1</sub> states of the tautomeric form plays an important role to determine the molecular-based tuning ESDPT. Therefore, it is of great importance to probe the proton-transfer tautomerism as a function of the relative excited-state thermodynamics for purine derivatives of which the electronic properties, depending on the functional group as well as substituted position, are altered.

**Acknowledgment.** This work was supported by National Science Council, Taiwan CNS (87-2119-M-194-002).

JA9917619

(11) 3MIBP was synthesized according to ref 12.<sup>12</sup> <sup>1</sup>H NMR(CDCl<sub>3</sub>, 200 MHz)  $\delta$  1.03 (d, 6H,  $J = 6.8$  Hz); 2.30–2.56 (m, 1H); 3.15 (d, 2H,  $J = 7.0$  Hz); 8.19 (s, 1H); 8.91 (s, 1H).

(12) Barlin, G. B.; Fenn, M. D. *Aust. J. Chem.* **1983**, *36*, 633.

(13) S<sub>0</sub>–S<sub>1</sub> ( $\pi\pi^*$ ) absorption onsets of the 7AI, 4ABI, and 6IBP dimers are taken to be 305, 292, and 275 nm, respectively (see Table 1).

(14) Cramer, C. J.; Truhlar, D. G. *J. Am. Chem. Soc.* **1993**, *115*, 8810.